

solution but can also be generated by ion molecule reactions, such as amines and other reasonably volatile neutrals. Quaternary ammonium ions completely disappear when a discharge is established. Ionized neutrals may still be observed.

Electrical discharge takes place very readily if the ES needle is at a negative potential with respect to the spray chamber, since field emission of electrons from a sharp point does not require a very high field. Electrons are eliminated by flushing the space around the spray tip with an electron scavenging gas such as oxygen (17) or SF<sub>6</sub>, or by the addition of a halogenated solvent to the liquid stream (18,19).

In a discharge, both positive and negative charge carriers are formed that will recombine with droplets having the opposite charge (20). As a result, droplet charge is neutralized and the formation of sample ions from charged droplets can no longer take place. Electrical discharge is prevented to a large extent by reduction of the electric field at the sprayer tip. Pneumatically or ultrasonically assisted ES works well at a lower electric field than pure ES.

### C. Flow Rate and Sensitivity

Electrospray is a low-flow-rate technique. When the flow rate is increased for a given sample concentration, the sample ion signal does not increase. So in terms of sample concentration, sensitivity remains constant, but in terms of mass flow, the sensitivity drops when the flow rate of the sample solution is increased. This is an unusual situation in mass spectrometry because a mass spectrometer operating in the electron ionization or chemical ionization mode is a mass-flow sensitive detector.

Apparent concentration sensitivity of ES can be attributed to a decrease in droplet charging efficiency and a shift toward larger diameters in the droplet size distribution if the liquid flow rate is increased. Both effects lead to a lower ionization efficiency. The reduced efficiency of the release of ions from droplets is approximately compensated for by the introduction of more sample molecules per unit time into the interface so that the signal level at the detector remains constant.

If the liquid flow rate is increased too much, the ion signals become lower and less stable. The practical upper limit to flow rate in pure ES is 10–20  $\mu\text{L}/\text{min}$ , depending on the composition of the solvent and on the use of a coaxial sheath flow (see Section I). Pneumatically assisted ES has been used up to 200  $\mu\text{L}/\text{min}$ . Manufacturers have claimed good performance of ultrasonically assisted ES up to 1 mL/min. High-flow ES is always combined with the supply of heat to assist evaporation of solvents. High-flow pneumatically assisted ES (ionspray) appears to require a heated zone in the source or a heated tube for the transport of ions from the source into the vacuum in combination with a so-called liquid shield (21). In a commercial embodiment of high-flow ionspray (called Turbo-Ion-Spray), the spray plume is mixed with a hot-air flow from a heat gun in the region in front of the ion-sampling orifice of the source (22).

In ion sources based on the heated tube design by Chait and co-workers (23),

as used in Finnigan mass spectrometers, the tube temperature is raised in the case of high-flow operation. At low liquid flow rate, the desolvation of charged droplets takes place mostly inside the atmospheric pressure source region, and ions are drawn into the heated tube together with solvent vapor and gas supplied to the source. At high flow rate, not only desolvated ions but also charged aerosol is drawn through the tube. Desolvation of the aerosol inside the tube generates sample ions that are transported into the mass analyzer, but nonvolatile material may be deposited inside the tube and eventually block the tube.

High-flow ES is compatible with 2-mm and wider bore columns in liquid chromatography. The need for eluent splitting is eliminated, but at the same time the load of nonvolatile contaminants on the ion source or transfer tube is much higher. All in all, it is probably better to feed a low flow rate into the sprayer and use a splitter, unless a gain in sensitivity at high flow can be substantiated, or the complexity of a splitter has to be avoided. A splitter can be set up using two capillary tubes of different length and diameter. At a given pressure drop, the flow rate through a capillary is proportional to the fourth power of the diameter and inversely proportional to the length of the capillary. A 1-m long 50- $\mu\text{m}$  i.d. transfer line together with a 16-cm long, 100- $\mu\text{m}$  side arm gives a split ratio of 1 : 100.

#### D. Position of the Sprayer Inside the Source

In the first published report of successful ES mass spectrometry (13), the spray capillary was positioned in the center of the source, in front the ion-sampling orifice of the ion source. When the experiments were repeated in Henion's group at Cornell University, the ion source of the SCIEX mass spectrometer was fully open and allowed the sprayer to be moved around during full operation. By moving to an off-axis position, the ion signal observed by the mass spectrometer was more stable, and at least as high as in the on-axis position (Fig. 6). It is desirable to take ions, but no droplets, into the mass analyzer. Charged droplets transported into the mass spectrometer may impinge on elements of the ion optics or mass analyzer and create bursts of ions that appear as spikes in the mass spectra. In the core of the aerosol generated by ES, the droplet diameter is larger than in the perimeter of the spray. Liberation of sample ions from small droplets should be more effective in the perimeter than in the core of the spray. There is more chance of incomplete droplet desolvation in the core of the spray than in the perimeter.

Off-axis positioning can be taken a step further by placing the sprayer in a diagonal position inside the source. The spray is not aimed at the sampling orifice, but at a position 1 cm beyond, in order to reduce the chance of shooting droplets into the mass spectrometer. Diagonal positioning is most effective for pneumatically assisted ES and is called "articulated ion spray." Stability is improved without loss of sensitivity.

Pure ES without pneumatic or ultrasonic assistance is more limited in freedom of positioning than the assisted sprays. The distance and voltage difference

## II. ELECTROSPRAY CONSTRUCTION AND OPERATION 117

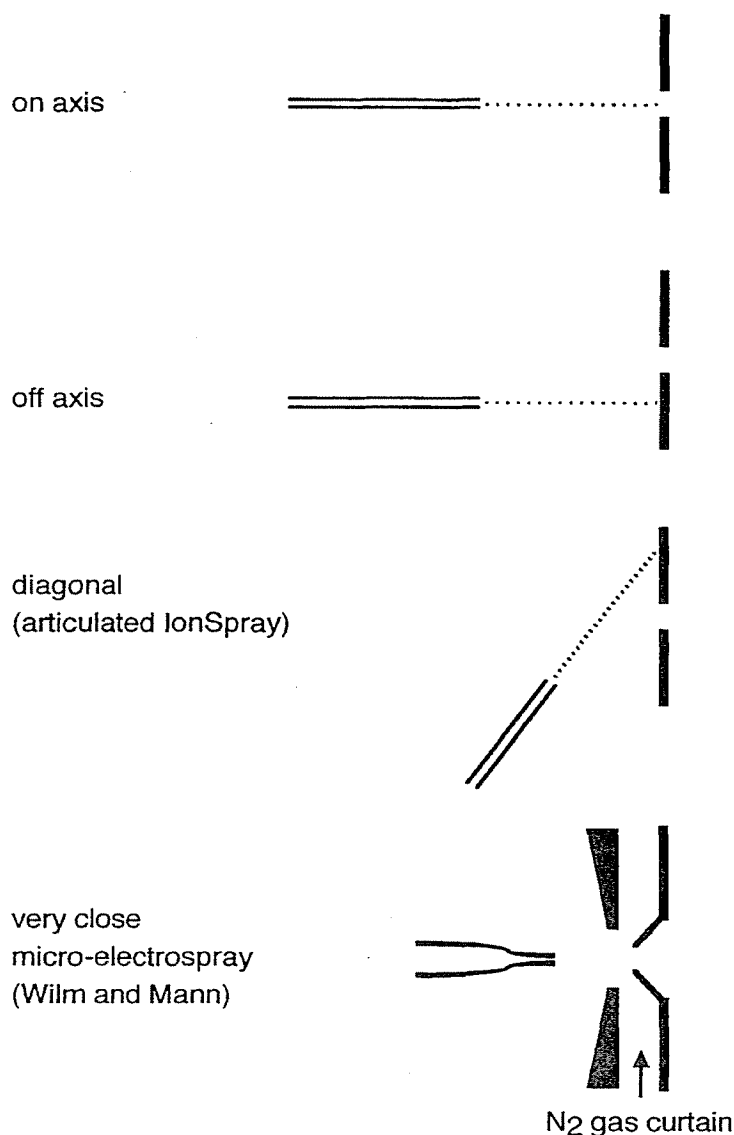


**Figure 6.** Arrangements for the position of the ES capillary in the ion source.

between the tip of the sprayer and the nearest part of the source determine the electric field that creates the spray and influences the performance of the spray. Optimization of position and spray voltage are interrelated.

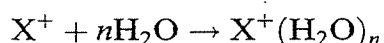
In the case of pneumatically and ultrasonically assisted ES, the aerosol generation is determined by gas flow or ultrasonic vibration. The electric field has limited influence on the spray. Aerosol generation is independent from the position of the sprayer in the source. Optimization of sprayer position is sample dependent. The best sprayer position for pneumatically assisted ES of proteins is closer to the sampling orifice and in a narrower region than the best position for small molecules.

An important difference exists between regular and micro ES. In regular ES, the distance between the tip of the sprayer and the ion-sampling orifice of the mass spectrometer is around 1 cm, in pneumatically assisted ES it is 2 cm, or more, combined with a spray voltage of a few kilovolts, but in micro ES the capillary is positioned exactly on axis and the distance from the ion-sampling orifice is reduced to a few millimeters, with concomitant reduction of the spray voltage (12) (Fig. 6).

### III. ATMOSPHERIC PRESSURE IONIZATION SOURCE CONSTRUCTION

#### A. Free Jet Expansion into Vacuum

Electrospray ionization is one of the ionization techniques available for an ion source operating at atmospheric pressure. Two problems are intimately related in atmospheric-pressure ionization (API) and ESMS: the transport of ions from an atmospheric pressure region into the vacuum system of the mass spectrometer, and the strong cooling of a mixture of gas and ions when expanding into vacuum. The resulting condensation of polar neutrals (notably water and solvent vapor) on analyte ions produces cluster ions having a mass far beyond the range of most mass analyzers.



A simple scheme of the expansion of a gas into a low pressure region is given in Figure 7A. The principles of the generation of molecular beams (24,25) will be explained in qualitative terms. Inside the nozzle opening and behind the nozzle the gas molecules gain a high velocity, and gas molecules with entrained ions follow straight stream lines originating approximately in the nozzle, the highest intensity of the gas flow being on the axis of the nozzle. Far away from the nozzle, the gas is pumped away, and gas molecules move at random. In the transition between directed motion and random motion, called shock waves, ions and gas molecules undergo many collisions, with scattering of the beam of ions and molecules as the result. The region inside the barrel shock wave, and between the nozzle and the Mach disk, is called the silent zone, where ions and gas move at equal speed in the same direction, and undergo strong and rapid cooling.

The location of the mach disk is important for the design of an API mass spectrometer. The distance from the nozzle is given by

$$x_M = 0.67D_o \sqrt{\frac{P_0}{P_1}}$$

where  $D_o$  is the orifice or nozzle diameter,  $P_0$  is the upstream (atmospheric) pressure, and  $P_1$  is the downstream pressure in the vacuum chamber (25). For a 0.1-mm nozzle diameter and  $10^{-5}$  Torr vacuum generated by cryogenic pump-

## III. ATMOSPHERIC PRESSURE IONIZATION SOURCE CONSTRUCTION

119

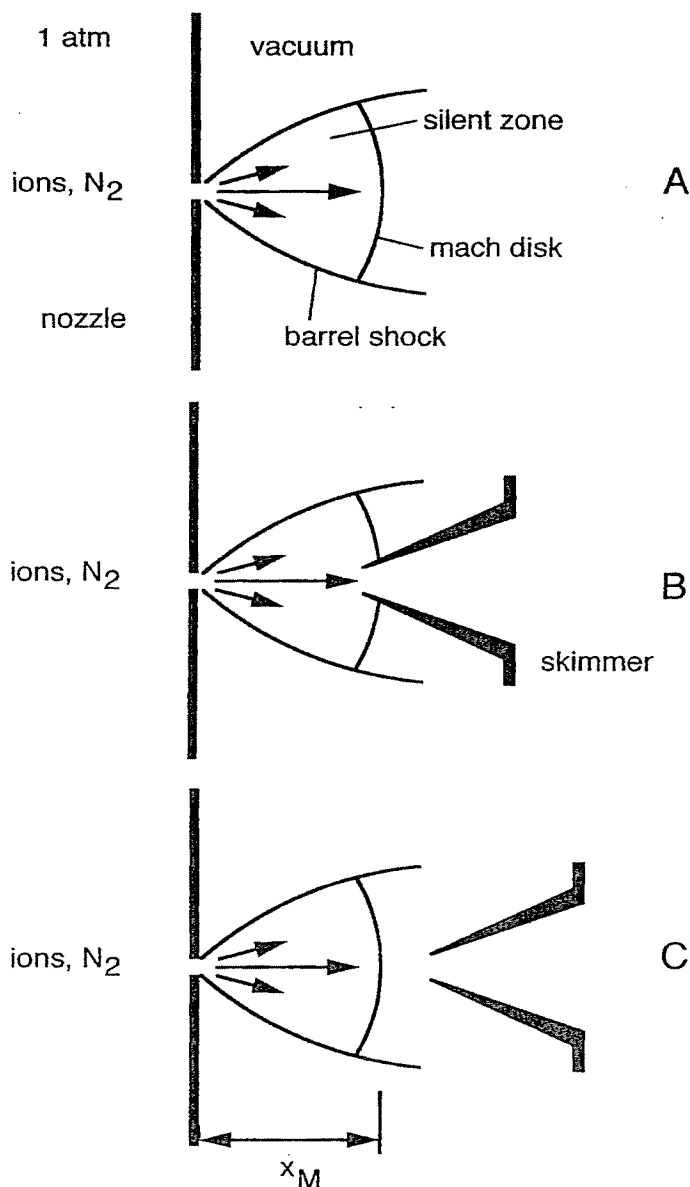


**Figure 7.** Free-jet expansion of gas and ions into vacuum; (A) basic principle; (B) arrangement with skimmer penetrating into the silent zone; (C) skimmer located more distant than the mach disk.

ing, the Mach disk is located at 670 mm, that is, beyond the dimensions of a quadrupole mass spectrometer. In an expansion through a 0.3-mm diameter orifice into a region pumped down to 1.2 Torr by a 35 m<sup>3</sup>/h rotary pump, the Mach disk is located at 5 mm from the nozzle opening and  $x_M$  is fully determined by the pumping speed available in the area near the nozzle opening. A small pump or narrow pumping line or other obstructions will result in a small  $x_M$ . A 16-m<sup>3</sup>/h rotary pump would have given  $x_M = 3$  mm. The gas flow through a

0.1-mm i.d. (or bigger) nozzle is too large for the turbomolecular or oil-diffusion pumps of the mass analyzer. Following the practice of molecular beam machines, the central portion of the beam can be sampled into the next vacuum stage by means of a skimmer (24,25), as depicted in Figure 7B and 7C. In Figure 7B, the core of the beam is sampled from the silent zone, and the ions plus gas continue their movement in straight lines. Collection of ions from the gas flow through the skimmer should be efficient, due to the directional effect of the free jet expansion. However, since the gas flowing in the molecular beam has strongly cooled upon expansion, ions will cluster with water molecules, if present.

In Figure 7C, a sample is taken from behind the Mach disk. Ions and gas have undergone extensive scattering, and the extraction and focusing of ions is more difficult. On the other hand, the gas temperature has risen through collisions in the Mach disk, with concomitant breaking of hydrogen bonds in cluster ions. The transmission of ions and gas through the skimmer is akin to the flow of ions and gas from a regular chemical ionization source. The circumference of the skimmer opening in Figure 7B should be very sharp and free from burrs. The full angle of the skimmer cone is usually about  $60^\circ$  in a molecular-beam apparatus (24,25) but can be wider in an API mass spectrometer. Fortunately, adequate transmission of ions instead of a beam of neutrals through the skimmer is subject to less-stringent conditions of mechanical quality of the skimmer.

## B. Cluster Ion Formation

In any design of an API mass spectrometer, the problem of the formation of cluster ions is addressed. Polar molecules that tend to cluster with ions are water and solvent vapor present in air or generated by the evaporation of the eluate from a liquid chromatograph or electrophoresis instrument connected to the API source. All practical designs of API instruments are aimed at either prevention of clustering, or at curing the problem by breaking the clusters.

**1. Prevention.** If ions are allowed, but water vapor and other neutrals can be excluded from entrance into the vacuum system, formation of clusters is prevented. This can simply be achieved by forcing ions and neutrals in opposite directions by the opposing action of an electric field and a flow of dry gas, usually nitrogen, as is customary in ion-mobility spectrometry. The flow of dry gas can be restricted to the area just in front of the ion-sampling orifice, but can also be extended to the entire ion source.

Figure 8A shows the essential part of the SCIEX API source. Ions are pushed toward the interface plate by the electric field from a corona discharge needle or ES capillary. The region between the interface plate and sampling orifice plate is continuously flushed with dry nitrogen. Part of the nitrogen flow goes to the left into the ion source, pushing water, neutral contaminants, and dust away from the sampling orifice. Ions that come close to the interface plate are driven to the right, toward the sampling orifice, by a 600-V potential difference between the

## III. ATMOSPHERIC PRESSURE IONIZATION SOURCE CONSTRUCTION

121

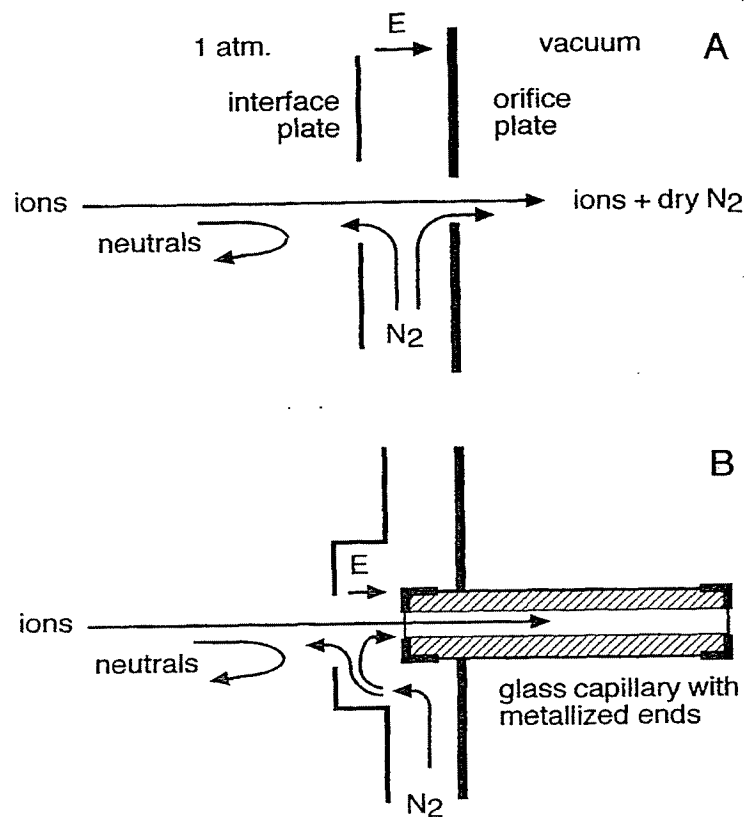


**Figure 8.** Prevention of cluster-ion formation and protection of sampling orifice or tube by means of: (A) gas curtain (SCIEX), (B) counter current flow of bath gas (Analytica of Branford).

interface plate and the orifice plate. The other part of the nitrogen flow goes through the sampling orifice, and carries sample ions into the vacuum of the mass analyzer. Ions have thus passed through a so-called dry nitrogen gas curtain. Clusters of ions and nitrogen are not formed, in spite of strong cooling during the expansion into the vacuum system, since nitrogen lacks the ability to form hydrogen bridges.

The countercurrent flow of nitrogen through the ES ion source developed by Fenn and co-workers (14) and built by Analytica of Branford for installation in Hewlett-Packard, Jeol, and other mass spectrometers is different in details, but serves the same purpose (see Fig. 8B). A curtain gas or countercurrent flow is a very elegant solution for the clustering problem. As a further benefit, the gas curtain largely avoids contamination and blockage of the sampling orifice, making the API source more reliable.

If the ion source is heated, the temperature of gas and ions remains high enough after the temperature drop resulting from the expansion, to prevent clustering.

Another way to preheat the mixture of ions and neutrals prior to expansion is via the heated transfer-tube system of Chait et al. (23). Ions and vapors pass through an approximately 20-cm long, 0.5-mm i.d. tube heated to 100–200°C.

The heated tube may also be used to help in the desolvation of ions contained in droplets. The source region itself can be at or above room temperature.

**2. Curing.** Ions pass through a region during the expansion into the vacuum, where the neutral gas density is falling rapidly. If ions moving in a low-density gas (pressure  $10^{-3}$  to 1 Torr) are accelerated by an electric field in this region, either between the nozzle and the skimmer or between the nozzle and the first ion optics element, collisions take place that lead to the breaking of hydrogen bonds in cluster ions. Such a declustering by collision-induced dissociation was described in an early study on corona discharges in air (26). Ten years later, declustering by CID was adopted by Kambara (27).

In an expansion system built according to Figure 7C, ions and gas pass through the Mach disk, where initially formed cluster ions are "heated" by collisions with randomly moving background gas. Water and solvent molecules will be partially removed from clusters and the mass spectrometer will show sample ions that may still be associated with a few water or solvent molecules. A disadvantage of this simple declustering method is that the collection of ions is less efficient owing to the scatter of the ion beam in the Mach disk.

Moderate acceleration of clusters is effective and widely used for declustering. The application of too much collision energy will not only strip off solvent molecules, but also lead to fragmentation of the sample ion.

### C. Focusing of Ions at Atmospheric Pressure

The very short mean free path and high collision rate at atmospheric pressure prevent classical ion focusing inside an atmospheric-pressure ion source. The geometry of the sampling orifice (flat or in a cone) and the dimensions and location of the lens or tube guiding a curtain gas (Fig. 8) are important for the ion-sampling efficiency. A correct combination of gas flow and electric field helps the guiding of ions toward the orifice. Careful attempts to drive ions to the orifice were made by Eisele (28). His aim was the sampling of very low concentrations of ions present in ambient air due to natural or other conditions. Ions were guided through a high-pressure ion optics region designed by computer simulation of electric fields. In spite of an extended electric field converging toward the sampling orifice, no increase in ion signals was observed. The conclusion was drawn that the electric field immediately in front of the sampling orifice was most important. Calculations and experiments by Sunner and co-workers (29,30) have shown that electric fields in the atmospheric pressure-ionization region are mainly dominated by space charge.

### D. Vacuum System Design

Electrospray API instruments can be divided into single-stage vacuum systems and multiple-stage vacuum systems. A single-stage instrument is shown schematically in Figure 9. Ions flow from the sampling orifice through ion optics into

## III. ATMOSPHERIC PRESSURE IONIZATION SOURCE CONSTRUCTION

123

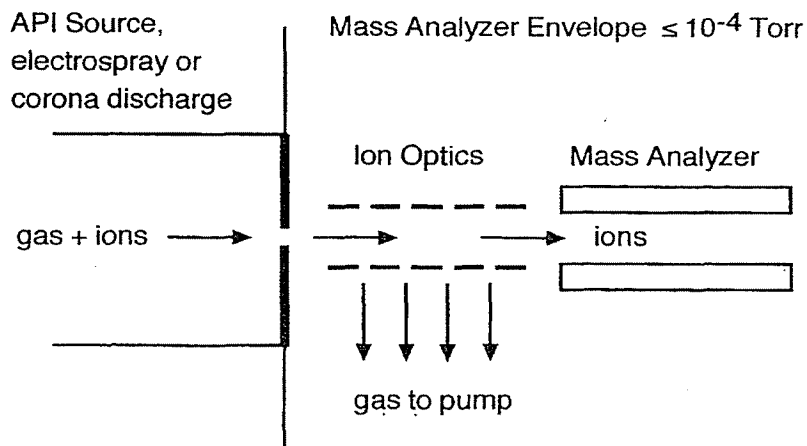


**Figure 9.** Electrospray (atmospheric pressure ionization) source with single stage vacuum system for the mass analyzer.

the mass analyzer. The ion optics stage can be either a stack of regular lenses or an RF only quadrupole (hexapole, octapole). The pressure tolerated by the mass analyzer sets the upper limit to the vacuum in the mass spectrometer. This pressure, together with the speed of the vacuum pump, sets the upper limit to the throughput of gas, and thus to the size of the sampling orifice. The higher the gas throughput, the more ions are transported through the sampling orifice. In older API instruments, a 10–25  $\mu\text{m}$  diameter orifice compatible with a 1000-L/sec oil diffusion pump was used. A high-sensitivity, single-stage atmospheric pressure-ionization instrument built by SCIEX makes use of a 120- $\mu\text{m}$  orifice protected by a gas curtain, combined with pumping by cryogenic surfaces surrounding the ion optics and quadrupole mass analyzer, rated at 100,000 L/sec.

High-speed cryogenic pumping is good from a theoretical point of view and has afforded very reliable performance in practice, but needs a big and expensive helium compressor. Manufacturers and researchers prefer a multiply staged vacuum system that can be built with less expensive vacuum pumps (Fig. 10). Ions are drawn through a sampling orifice into a first chamber, pumped to approximately 1 Torr by a rotary pump. Part of the expanding beam of gas and ions is taken into the second chamber, pumped down to  $10^{-2}$  Torr or less. Most of the gas is pumped away in the second stage and a suitable ion-optics arrangement guides the ions into the mass analyzer region, which is pumped down to  $10^{-5}$  Torr. The second and third stages are usually the original source housing and analyzer housing of a standard differentially pumped mass spectrometer designed for chemical ionization. This simple scheme may be elaborated in different ways, to comply with particular geometrical or electrical constraints. In recent implementations of the multiple-stage vacuum system the first or the second stage has been split in two, which increases the total number of stages to four.

Multiple-stage vacuum systems use a larger orifice, which can take more gas and ions into the first vacuum stage of the mass spectrometer. Unfortunately a

## 124 ESI SOURCE DESIGN AND DYNAMIC RANGE CONSIDERATIONS

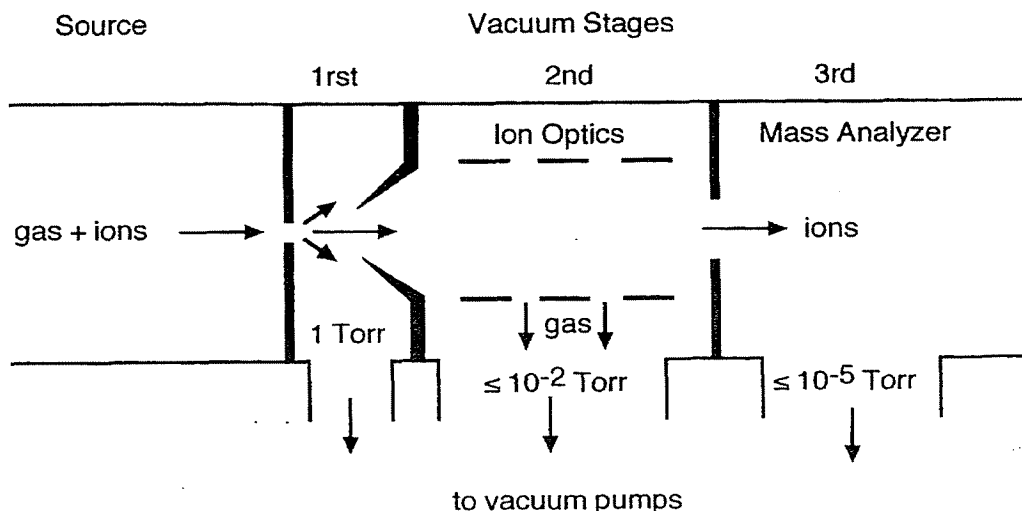


**Figure 10.** Vacuum system with multiple stages: 1st stage, free-jet expansion, molecular-beam stage; 2nd stage, ion optics; 3rd stage, mass analyzer.

large throughput through the sampling orifice and high sensitivity do not always go hand in hand. In a discussion about sensitivity, the first vacuum stage in Figure 10 will be called the molecular-beam stage, the second the ion-optics stage, and the third the analyzer stage.

For simplicity, we assume that no significant enrichment of heavy ions over light gas molecules takes place during passage through the first vacuum stage into the skimmer. We assume that the ion-optics region is transparent to neutrals that are removed by the first high-vacuum pump. We also assume that no ions are lost during transport through the ion-optics region. In short then, the ions to gas ratio is significantly increased in the ion-optics stage.

Typical orifice dimensions are 0.3–0.5 mm for the nozzle combined with 1.4–0.6 mm for the skimmer. The best transmission of ions is achieved when the skimmer penetrates into the silent zone of the free jet expansion so that the ion-optics stage receives a well-shaped ion beam. In attempts to build ES API sources for magnetic sector instruments, the addition of a fourth pumping stage appeared advantageous. Problems with sector instruments are arcing due to the high voltage on the ion source, electrical discharges in pumping lines, and collisions between ions and background gas in the acceleration region. Manufacturers appear to have overcome such problems. Strict adherence to molecular-beam rules may not be necessary, since the more efficient extraction of ions from an ion source in a sector instrument may offset the disadvantage of scattering of ions in intermediate pressure regions.

### E. Vacuum System and Sensitivity

The goal for the design of the system for ion transport from the ES source into the mass analyzer is to introduce as many ions, but as little gas, as possible.

Ideally, ions should be separated from gas. In a simple approximation, the sensitivities of different API mass spectrometers can be judged from the throughput of gas in the relevant vacuum stage (31). In a single-stage vacuum system, the flow of ions into the mass analyzer is proportional to the gas flow through the sampling orifice. The throughput of gas into the analyzer is given by the pumping speed multiplied by the pressure in the vacuum system.

For 1000 L/sec and  $10^{-5}$  Torr we obtain 0.01 Torr.L/sec. If the single-stage system is equipped with a 100,000 L/sec cryopump, the throughput is increased to 1 Torr.L/sec (SCIEX API 3). The sensitivity is increased by the same factor of 100.

In the discussion of multiple-stage vacuum systems, we assume for simplicity that an ion-optics stage transmits all ions toward the mass analyzer, while gas is pumped away, thereby increasing the ions to gas ratio; a molecular beam stage is supposed to transfer a portion of the gas plus ion beam, without changing the ions to gas ratio. However, recent versions of the molecular beam stage include a tube lens or focusing ring or focusing cone for increasing the ions to gas ratio as shown in Figure 11 (32). Positive ions that have spread out during the free-jet expansion are forced back toward the center through the skimmer by the application of a positive voltage on the tube, ring, or cone. A negative voltage is used for negative ions. Sensitivity is increased by a factor of 2–5, depending on the geometry. The ion-optics stage may be equipped with lenses, an RF-only quadrupole (hexapole, octapole) or other elements.

In a three-stage system, the first stage does not dramatically increase the ions to gas ratio. The ion optics stage is crucial, and with a 1000 L/sec pump and  $10^{-3}$  Torr (approximate values for our NERMAG R3010 triple quadrupole with homemade source) a throughput of 1 Torr.L/sec can be obtained. Sensitivity roughly equal to the SCIEX API 3 instrument is obtained, at the expense, however, of some backstreaming of diffusion pump oil into the ion-optics region. In all instruments built along these lines, the pumping and pressure in the ion-optics stage determine the sensitivity. A compromise on pumping will compromise sensitivity. It has appeared that the efficiency of ion transport through an RF-only quadrupole (hexapole, octapole) increases if the pressure is raised to approximately  $10^{-2}$  Torr (33). To obtain the same gas throughput, a smaller pump can be used. At  $2 \cdot 10^{-2}$  Torr, and 50 L/sec, the throughput is again 1 Torr.L/sec. At this high pressure, it becomes difficult to select the right vacuum pump. Diffusion pumps cannot be used at an inlet pressure above  $2 \cdot 10^{-3}$  Torr, and suffer from considerable backstreaming of diffusion pump oil. Turbomolecular pumps have reached their limits at  $10^{-2}$  Torr, and  $8 \cdot 10^{-3}$  Torr appears a practical value for a 50 L/sec turbomolecular pump. A new development is a dual-inlet turbomolecular pump, equipped with a high-pressure port for pumping the RF-only quadrupole, and a regular low-pressure inlet port for pumping the mass analyzer (34).

The prediction of sensitivity based on vacuum considerations alone is a first approximation. The effects of the quality of the molecular-beam components, ion optics, and mass analyzer cannot be included in a simple generalization. The

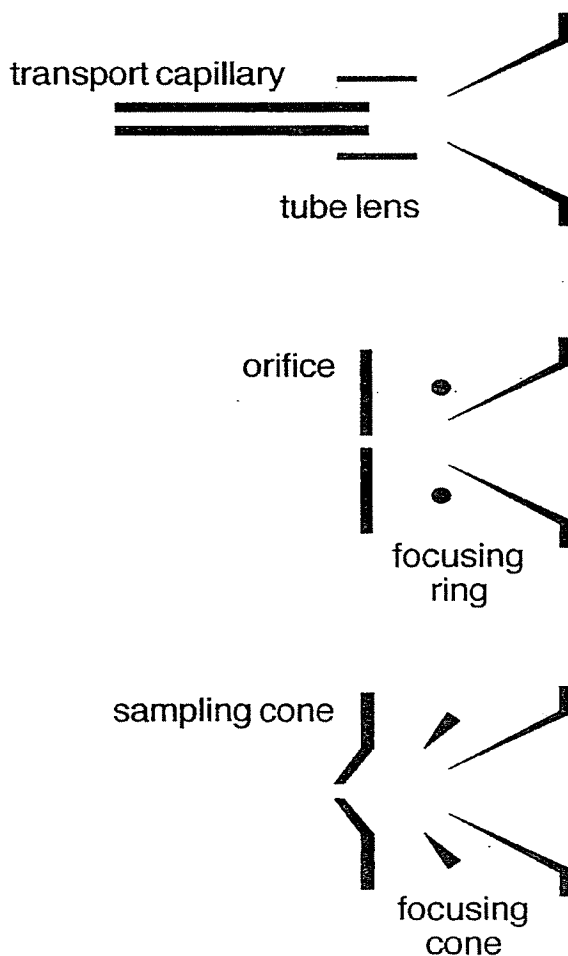


**Figure 11.** Tube lens (Finnigan), ring (SCIEX), or cone (Micromass) located in the molecular beam stage for forcing ions through the skimmer orifice.

atmospheric part of the ES source on each vacuum system was assumed to be equally efficient in each case. A comparison between different instrument designs would require running the same sample in different instruments under well-defined and carefully controlled conditions.

#### F. Ion-Sampling Orifice

Various arrangements of the sampling orifice are given in Figure 12. A hole in a disk (*a*), in the top of a cone (*b*), or in the bottom of an inverted cone (*c*) can be used equally well. A 20-cm long  $\times$  0.5 mm i.d. glass tube (*d*) or heated metal tube may also be used instead of an orifice.

The formation of molecular beams from nozzles of various shapes has been reported (35). Campargue recommends a short straight capillary with a ratio of

## III. ATMOSPHERIC PRESSURE IONIZATION SOURCE CONSTRUCTION

127

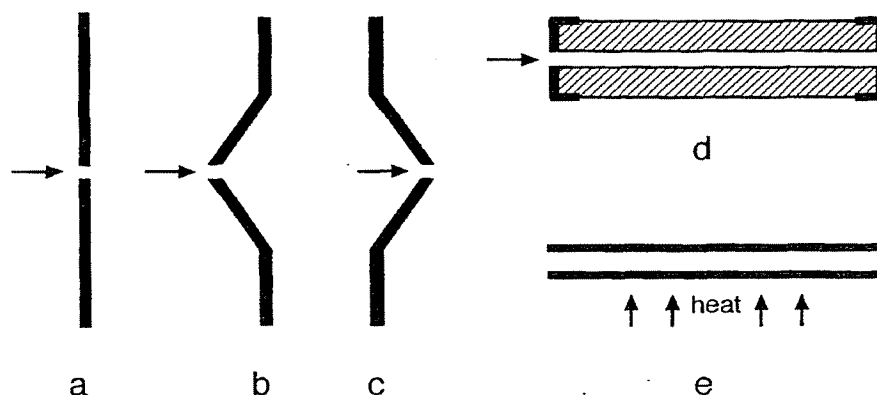


**Figure 12.** Sampling of ions and gas from the atmospheric-pressure ionization source via different shapes of orifices and tubes; (a) orifice in a flat disk (SCIEX API 100/300); (b) orifice in the top of a cone (Micromass, SCIEX API 3); (c) orifice in the bottom of a cone (Vestec); (d) glass tube with metallized ends (Analytica source customized for HP, Jeol, Bruker, and others), (e) heated metal tube (Finnigan MAT).

length to diameter equal to or greater than 2 (25). In our hands, a 0.3-mm diameter hole in a flat 1.0-mm thick stainless-steel disk and protected by a gas curtain has proven very robust and reliable in experiments with corona discharge ionization or ES during the past seven years. The operation of an API source at any desired voltage, independent of the mass analyzer, has advantages for magnetic sector instruments and for certain liquid-sample inlet systems. The transport of ions through a glass capillary instead of a metal nozzle gives the desired insulation, as discussed earlier in this chapter. The flat ends of the capillary are metal plated for efficient sampling of ions into the capillary and acceleration of ions at the exit. The gas flow drags ions through the capillary into the vacuum system, even if the electric field existing between the metallized ends opposes such a transport. Chait et al. have used a long heated metal capillary for the desolvation of ions from charged microdroplets generated by ES and introduction of the core ions into a quadrupole mass spectrometer. Another purpose served by the capillary is the transport of ions over a longer distance (e.g., 20 cm) between the API source and the ion optics and acceleration region of the mass analyzer, giving more freedom in mechanical construction.

Ion-transport efficiency through capillary tubes has been studied in detail by Lin and Sunner (36) and by Guevremont and co-workers (37). Transmitted currents were very similar for glass and metal capillaries (36). It was more difficult to obtain stable and reproducible transmitted currents with glass than with metal capillaries. Experiments were made with very long (0.6–15 m) capillaries, so that shortcomings observed are probably more pronounced than in real life in mass spectrometry, where the capillary length is 20 cm or shorter.

Contamination of the sampling orifice or tube can be troublesome. The

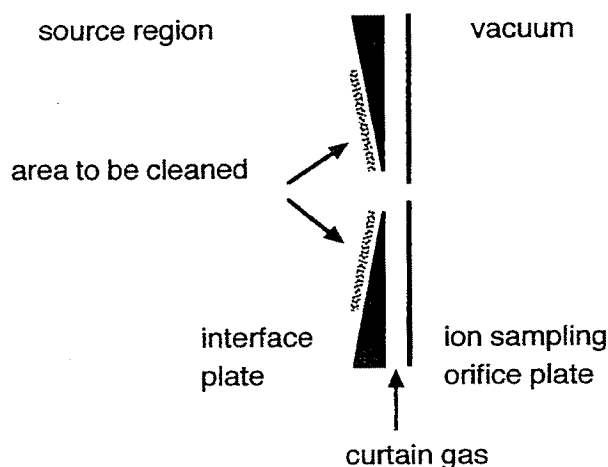
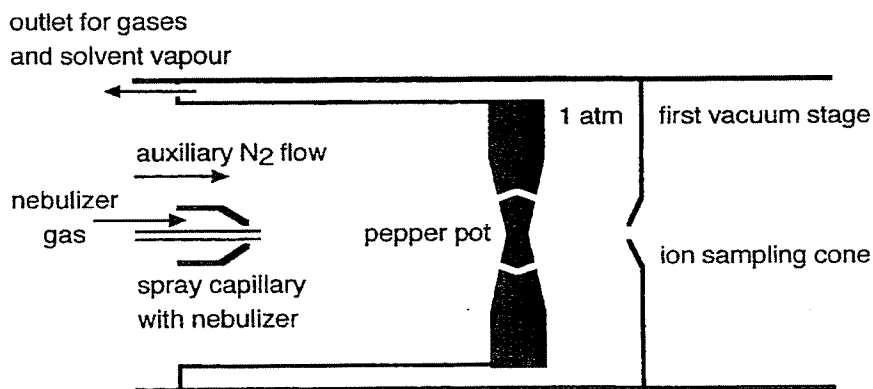


Figure 13. Area to be cleaned inside the atmospheric pressure-source region.

buildup of charge on a layer of contaminants inside an orifice or tube can effectively stop the passage of ions, while the flow of neutrals (as read from vacuum gauges) is not affected. An ES source should be designed for ease of removal and cleaning of the orifice or tube. The orifice in our instrument (0.3 mm i.d. in a 1-mm thick stainless-steel disk) can be cleaned with a sharp pin of wood and aluminium oxide powder followed by sonication in ethanol. Depending on the operating conditions, cleaning takes place after one or two months of use. Surprisingly, it has never been necessary to clean the skimmer. Tubes are less easy to clean. Blockage of a tube or orifice is prevented by the use of a gas curtain. Foolproof operation cannot be guaranteed. One should be careful and avoid spraying straight at the orifice or tube since droplets can penetrate through the gas curtain. As discussed above, off-axis or diagonal positioning not only increases stability and abundance of ion signals, but also helps to prevent contamination of the sampling orifice (nozzle) or tube. If such precautions are taken together with protection by a gas curtain, it is possible to use nonvolatile buffer components in CE/MS, or use post-column addition of a dilute sodium chloride solution in LC/MS to promote formation of  $M.Na^+$  ions of polar neutral samples such as sugars. The area around the sampling orifice needs periodic cleaning (Fig. 13). Fields created by charges on contaminating layers may disturb the electric field in front of the sampling tube or orifice and prevent ions from being entrained in the gas flow into the vacuum.

Micromass instruments are equipped with a so-called pepper pot located in the atmospheric pressure region between the sprayer tip and the sampling orifice (Fig. 14). The pepper pot eliminates a line of sight between the sprayer and the sampling orifice (called sampling cone by Micromass) and reduces contamination of the orifice. Ions and small charged droplets pass through the holes in the pepper pot, while relatively big droplets impinge on the front and inside walls of



**Figure 14.** Pepper pot for reduction of contamination of the sampling cone in Micromass mass spectrometers.

the channels. Since the source is heated, the pepper pot also aids in the transfer of heat to droplets, solvent vapor, and auxiliary gases in the source.

#### G. Ion Optics Between Sampling Orifice and Mass Analyzer

In the space between the sampling orifice (or outlet of sampling tube) and skimmer, ions are transported in the free-jet expansion of gas. Part of the beam of ions and gas passes through the skimmer into the next vacuum stage. Effective focusing of ions into a very narrow beam is not possible, but ions can be forced to remain closer to the axis of the beam if a tube or ring is positioned between nozzle and skimmer (32). A positive voltage on the tube lens or ring reduces the spreading of positive ions away from the axis. The gain in sensitivity is between two- and fivefold.

Behind the skimmer the pressure is lower, but still not low enough for effective focusing with ion lenses. RF-only quadrupoles, hexapoles, and octapoles are now preferred by most manufacturers of quadrupole and magnetic-sector mass spectrometers to guide ions into the mass analyzer section. Douglas has observed that the efficiency of guiding ions is significantly increased if the pressure is raised to  $10^{-2}$  Torr (33). Collisions between ions and background gas keep the ions on a path close to the quadrupole axis, in the same manner as ions are confined to the center of a quadrupole ion trap by collisions in  $10^{-3}$  Torr of helium. Ions are slowed down by collisions in the RF-only quadrupole and enter the next stage with a limited energy spread of a few electron volts. Ion transmission from the RF-only multipole into the mass analyzer is easier and focusing much less dependent on mass.

The occasional penetration of charged droplets into a quadrupole mass analyzer shows up as random spikes in mass spectra. Off-axis positioning of the sprayer can reduce this aerosol noise. In Finnigan TSQ and SSQ mass spectrometers the skimmer is positioned slightly off axis. Since heavy aerosol

particles follow a straight line on the axis of the ion transfer tube, they impinge on the outside wall of the skimmer. A sizable fraction of ions deviates from the center and is passed through the skimmer. Noise is eliminated, at the expense of a reduction in ion transmission.

Ion-counting detection is more immune to spikes of this nature when compared with analog current measurement, because a burst of *many* ions arriving together at the electron multiplier is recorded as *one* pulse by the ion-counting detector, while the same burst is amplified to a large voltage spike by the current-to-voltage converter of an analog detector.

#### IV. UP-FRONT COLLISION-INDUCED DISSOCIATION

Electrospray mass spectra are usually devoid of fragment ions. Fragments can be formed in a triple quadrupole, in an ion trap, ICR cell, or in the field-free regions of magnetic-sector mass spectrometers.

In atmospheric-pressure ionization mass spectrometry, including ES mass spectrometry, fragmentation can easily be induced in one of the higher-pressure regions of the ion passageway from the source into the mass analyzer. Acceleration of ions between nozzle (tube) and skimmer by  $\Delta V(N-S)$  or between skimmer and RF-only multipole by  $\Delta V(S-Q)$  results in collisions of ions with gas in which ions are entrained in their flow into the vacuum (Fig. 15). Sometimes this process is called "in-source CID" which is clearly a misnomer. Further

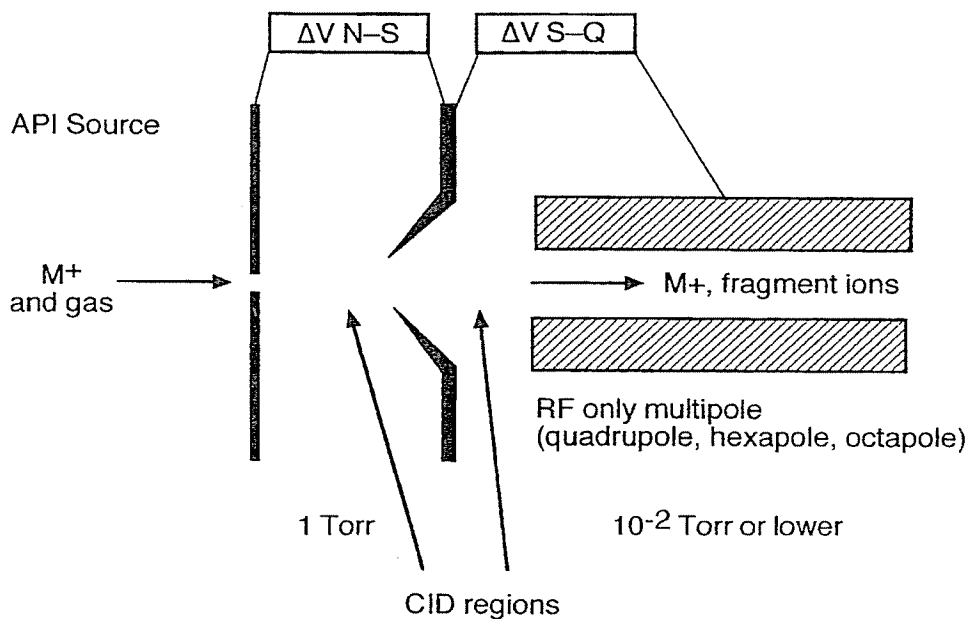


Figure 15. Collision-induced dissociation just outside the ion source.

confusion is created by the use of different names for the same process by users and manufacturers: nozzle-skimmer fragmentation, cone-voltage fragmentation, high-orifice potential fragmentation, and octapole fragmentation, to name a few.

Fragment ions produced by collision-induced dissociation are very efficiently transported into the mass analyzer. The major advantage of this poor man's MS/MS method is its simplicity: only one voltage has to be increased, no switching and adjustment of collision gas and retuning of ion optics is necessary. Of course, there is no parent ion selection possible. In LC/MS one can do one LC run without CID, and one with CID to obtain fragments of all components. An elegant application of up-front CID in LC/MS is stepping the CID (orifice) voltage during the course of each mass spectrum: a high voltage is used in the low-mass region, to generate and detect low-mass fragments, while the voltage is reduced again at, for example,  $m/z$  200 and above, in order to collect unfragmented parent ions (38). Phosphorylated peptides were selectively detected in LC/MS of an enzymatic digest of a phosphoprotein.

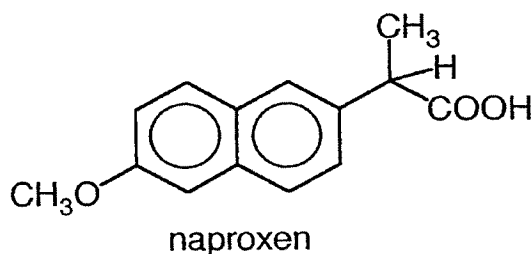
Since up-front CID takes place just *outside* the ion source, it can be combined with any ionization technique that is applicable in atmospheric pressure-ion sources. In Figure 15 the accumulated effect of  $\Delta V(N-S)$  and  $\Delta V(S-Q)$  can lead to fragmentation. CID takes place under the condition of sufficient translational energy and gas density. In a magnetic-sector instrument, the residual gas density in the accelerating region may be high enough for CID. An additional pumping stage is used by manufacturers to eliminate unwanted CID in the accelerating region.

Mild up-front CID reduces the abundance of background ions, a distinct advantage for LC/MS or CE/MS where the contribution of background ions to the baseline noise in the total ion current trace is a serious problem. In multiply staged instruments, the transmission of ions is improved if the  $\Delta V(N-S)$  is increased, in particular for big protein ions. In fact, it is not too difficult to achieve good transmission of protein ions without inducing fragmentation, because collision energy is partitioned over a large number of vibrational degrees of freedom. It is not as easy to obtain good transmission of small molecules that fragment much more easily. Manufacturers that jumped into ES with molecular-weight determination of proteins as their first goal discovered that good sensitivity for small molecules, notably pharmaceuticals and labile drug conjugates, is a different game.

In a well-designed API mass spectrometer, the abundance of a sample ion at  $m/z$  200–300 decreases very little if  $\Delta V(N-S)$  is reduced from 50 V down to a few volts. A good test compound for unwanted CID is the drug naproxen. At low collision energy, the negative-ion ES spectrum shows the  $[M-H]^-$  ion at  $m/z$  229 as the only peak. It should be easy to adjust  $\Delta V(N-S)$  and  $\Delta V(S-Q)$  for a spectrum free from fragment ions. Already at a moderate collision energy, where most sample ions would survive, the  $[M-H]^-$  ion loses  $CO_2$  so easily that  $m/z$  185 becomes the base peak. In the positive-ion mode, the  $M.H^+$  ion of dibutyl phthalate at  $m/z$  279 can be used as a test ion. Fragmentation to  $m/z$  149

## 132 ESI SOURCE DESIGN AND DYNAMIC RANGE CONSIDERATIONS

is easy, but does not take place as readily as the loss of  $\text{CO}_2$  from  $m/z$  229 of naproxen.



Removal of the last solvent molecule(s) from a sample ion by up-front CID may not be possible without unintended fragmentation of a labile sample ion

## V. MASS-SCALE CALIBRATION

Calibration of the mass scale requires a series of ions evenly spaced throughout the mass range. Ideally, the calibrant should be easily removed from the source and leave no traces in the source or liquid-handling system. Mixtures of a protein (usually myoglobin) and some smaller peptides can be used; polyethylene glycols and polypropylene glycols are also widely used for calibration. Anacleto et al. have summarized different options, and have proposed protonated water clusters and salt clusters (39), generated by pneumatically assisted ES. Water clusters provided a calibration range up to  $m/z$  1000 in the SCIEX API III mass spectrometer. Alkali metal halides (sodium iodide) allow calibration on cluster ions  $\text{Na}^+(\text{NaI})_n$  or  $\text{I}^-(\text{NaI})_n$  up to  $m/z$  2400, the full mass range of this instrument.

In principle, mass-scale calibration is independent of the ionization technique. During the past seven years, we have routinely calibrated by the use of a combination of corona discharge and controlled cluster formation in the free-jet expansion. Corona discharge of the headspace of an aqueous ammonia solution creates  $\text{NH}_4^+(\text{H}_2\text{O})_n$  with  $n = 0-4$  after passage through the gas curtain. If the curtain gas flow is reduced but not cut off, one can tune the gas flow to allow a controlled amount of moisture into the free-jet expansion so that a complete series of  $\text{NH}_4^+(\text{H}_2\text{O})_n$  ions is formed that extends all the way up to  $m/z$  2000 (mass range of a NERMAG R3010) and most probably beyond this value. The calibration mass series starts at  $m/z$  54, and one out of every five clusters is used, giving a calibration mass separation of 90 amu. The relatively low abundance of deuterium and  $^{17}\text{O}$ , and the higher abundance of  $^{18}\text{O}$  in the cluster ions, makes this calibrant suitable for resolution adjustment on isotope peaks.

## VI. DYNAMIC RANGE IN ELECTROSPRAY

When the concentration of a sample in solution is increased, the abundance of sample ions created by ES increases until a plateau is reached. A limited dynamic range is a serious drawback in analytical applications of ES ionization mass spectrometry. The upper limit to the usable concentration range is dependent on the sample itself and on the presence of other charged material, such as electrolytes or buffers in the sample solution. Tang and Kebarle have measured the amount of charge on droplets (the spray current) and sample ion abundance as a function of concentration of a sample dissolved in reagent-grade methanol. They rationalized the upper limit as the result of interplay between droplet charging on the one hand and the competition between sample ions and background electrolyte ions leaving the charged droplets on the other hand. A close relationship between the dynamic range limit at  $10^{-5}$  M sample concentration and the estimated  $10^{-5}$  M background ion concentration was proposed (40). In short, the upper limit was attributed to competition of ions for insufficient charge on droplets.

In our hands, the same upper limit of  $10^{-5}$  M was found for tetrabutylammonium bromide dissolved in the highest-purity gradient-grade solvents, introduced into the ES source via repeatedly, rigorously cleaned components. The spray current keeps rising with increasing sample concentration above  $10^{-5}$  M, while the ion signal reaches a plateau. Limitations in ion transport or in the spray process were ruled out (41). Measurement of the current arriving at the skimmer showed that the skimmer current also reaches a plateau at  $10^{-5}$  M, while the spray current keeps rising (42) (Fig. 16). One has to conclude that above  $10^{-5}$  M an increasing amount of charge on droplets cannot be converted into sample ions. In other words, sample ions cannot escape from droplets.

A reasonable explanation is the complete filling of droplet surface with sample ions and sample molecules at  $10^{-5}$  M. More sample in solution would not give more sample at the droplet surface, and the upper limit to sample ion abundance is reached. This viewpoint can be supported by simple calculation and assumptions based on experiments on fission of charged droplets (43,44). Let us assume a primary droplet size of 1  $\mu\text{m}$  radius and fission into droplets of 0.1  $\mu\text{m}$  radius. Let us assume that sample ions and sample ion pairs all reside on the droplet surface, a reasonable assumption for surface-active quaternary ammonium salts, and an equally reasonable assumption for a good many organic compounds having a polar functional group. These small droplets have been separated from the surface of parent droplets and have the same density of sample at the surface as the parent droplets. The 0.1- $\mu\text{m}$  radius droplet shrinks by evaporation down to 10 nm, and emission of ions from the surface takes place; the numbers are given in Table 1. The bottom line is that a 10-nm radius droplet has about 5  $\text{nm}^2$  of droplet surface available per sample ion or sample molecule, whereas the surface taken by one sample ion is of the order of 3  $\text{nm}^2$ . The droplet surface is indeed almost full at  $10^{-5}$  M after droplet disintegration and evaporation.

An increasing amount of charge is not converted into sample ions. This

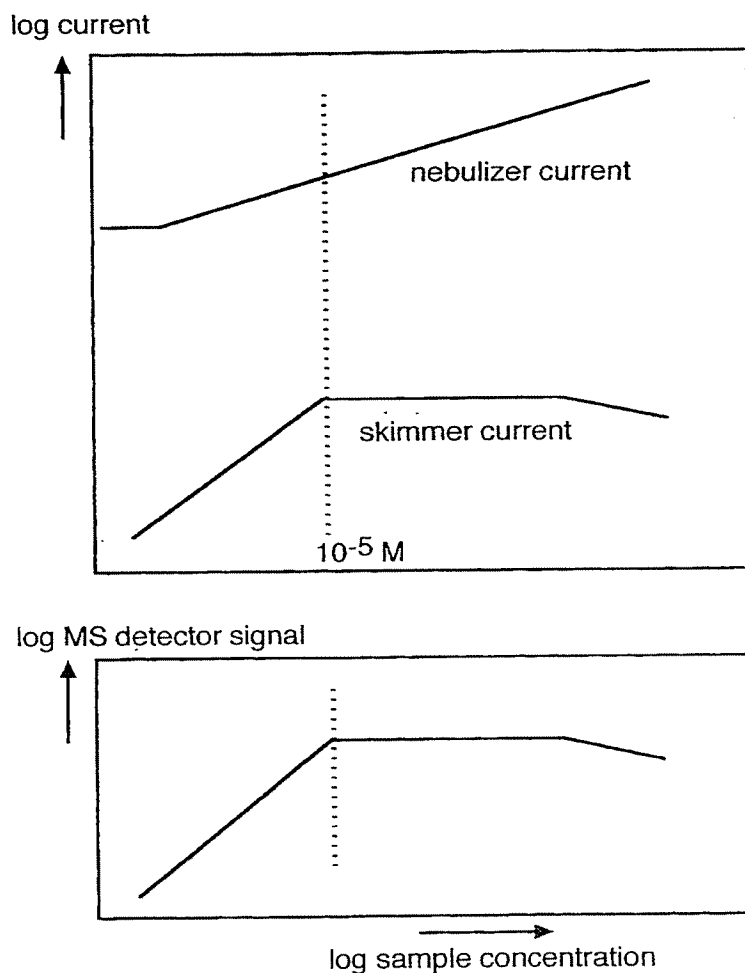


**Figure 16.** Nebulizer current, skimmer current, and ion signal as a function of sample concentration of tetrabutylammonium bromide dissolved in gradient-grade acetonitrile (95%) plus methanol (5%).

**TABLE 1.** Area Available on a Droplet Surface at  $10^{-5}$  M

Radius of initially formed droplet	$r = 1 \mu\text{m}$
Number of sample ions plus sample molecules	24,000
Area available per sample ion or molecule	$500 \text{ nm}^2$
After fission to	$r = 0.1 \mu\text{m}$
Surface density equal to parent droplet	
Area available per sample ion or molecule	$500 \text{ nm}^2$
Number of sample ions plus sample molecules	240
After size reduction by evaporation	$r = 10 \text{ nm}$
Area available per sample ion or molecule	$5 \text{ nm}^2$
Radius of average organic ion or molecule (C-C bond length 0.15 nm)	app. 1 nm
Area taken by one ion or molecule	app. $3 \text{ nm}^2$

unused charge probably resides in droplets that cannot release sample ions. It is unclear at present if developments in source design will alleviate the dynamic range problem.

## REFERENCES

1. Bailey, A. G. *Electrostatic Spraying of Liquids*; Electrostatics and Electrostatic Applications Series; Wiley: New York, 1988.
2. Smith, R. D.; Barinaga, C. J.; Udseth, H. R. *Anal. Chem.* **1988**, *60*, 1948–1952.
3. Mylchreest, I. C.; Hail, M. E. *United States Patent* 5,122,670; June 16, 1992.
4. Bruins, A. P.; Covey, T. R.; Henion, J. D. *Anal. Chem.* **1987**, *59*, 2642–2646.
5. Banks, J. F.; Shen, S.; Whitehouse, C. M.; Fenn, J. B. *Anal. Chem.* **1994**, *66*, 406–414.
6. Banks, J. F.; Quinn, J. P.; Whitehouse, C. M. *Anal. Chem.* **1994**, *66*, 3688–3695.
7. Hail, M. E.; Mylchreest, I. C. *United States Patent* 5,170,053; December 8, 1992.
8. Wahl, J. H.; Gale, D. C.; Smith, R. D. *J. Chromatogr.* **1993**, *659*, 217–222.
9. Kriger, M. S.; Cook, K. D.; Ramsey, R. S. *Anal. Chem.* **1995**, *67*, 385–389.
10. Gale, D. C.; Smith, R. D. *Rapid Commun. Mass Spectrom.* **1993**, *7*, 1017–1021.
11. Emmet, M. R.; Caprioli, R. M. *J. Am. Soc. Mass Spectrom.* **1994**, *5*, 605–613.
12. Wilm, M. S.; Mann, M. *Int. J. Mass Spectrom. Ion Processes* **1994**, *136*, 167–180.
13. Yamashita, M.; Fenn, J. B. *J. Phys. Chem.* **1984**, *88*, 4451–4459.
14. Whitehouse, C. M.; Dreyer, R. N.; Yamashita, M.; Fenn, J. B. *Anal. Chem.* **1985**, *57*, 675–679.
15. Larsen, B. S.; McEwen, C. N. *J. Am. Soc. Mass Spectrom.* **1991**, *2*, 205–211.
16. Cody, R. B.; Tamura, J.; Musselman, B. D. *Anal. Chem.* **1992**, *64*, 1561–1570.
17. Yamashita, M.; Fenn, J. B. *J. Phys. Chem.* **1984**, *88*, 4471–4675.
18. Cole, R. B.; Harrata, A. K. *Rapid Commun. Mass Spectrom.* **1992**, *6*, 536–539.
19. Hiraoka, K.; Kudaka, I. *Rapid Commun. Mass Spectrom.* **1992**, *6*, 265–268.
20. Whitby, K. T.; Liu, B. Y. H. in *Aerosol Science*; Davies, C.N., Ed.; Academic Press: London, 1966, Chapter III.
21. Hopfgartner, G.; Wachs, T.; Bean, K.; Henion, J.D. *Anal. Chem.* **1993**, *65*, 439–446.
22. Covey, T. R.; Anacleto, J. F. *United States Patent* 5,412,208; May 2, 1995.
23. Chowdhury, S. K.; Katta, V.; Chait, B.T. *Rapid Commun. Mass Spectrom.* **1990**, *4*, 81–87.
24. Anderson, J. B.; Andres, R. P.; Fenn, J. B. in *Adv. At. Mol. Phys.*, Bates, D. R.; Estermann, I. Eds.; Academic Press: New York, 1965, Chapter 8.
25. Campargue, R. *J. Phys. Chem.* **1984**, *88*, 4466–4474.
26. Shahin, M. M. *J. Chem. Phys.* **1966**, *45*, 2600–2605.
27. Kambara, H.; Kanomata, I. *Anal. Chem.* **1977**, *49*, 270–275.
28. Eisele, F. L. *Int. J. Mass Spectrom. Ion Processes* **1983**, *54*, 119–126.
29. Busman, M.; Sunner, J. *Int. J. Mass Spectrom. Ion Processes* **1991**, *108*, 165–178.
30. Busman, M.; Sunner, J.; Vogel, C. R. *J. Am. Soc. Mass Spectrom.* **1991**, *2*, 1–10.
31. Bruins, A. P. *Mass Spectrom. Rev.* **1991**, *10*, 53–77.

## 136 ESI SOURCE DESIGN AND DYNAMIC RANGE CONSIDERATIONS

32. Mylchreest, I. C.; Hail, M. E.; Herron, J. R. *United States Patent* 5,157,260; October 20, 1992.
33. Douglas, D. J.; French, J. B. *J. Am. Soc. Mass Spectrom.* **1992**, 3, 398–408.
34. Balzers model TMH 260–130.
35. Murphy, H. R.; Miller D. R. *J. Phys. Chem.* **1984**, 88, 4474–4478.
36. Lin, B.; Sunner, J. J. *Am. Soc. Mass Spectrom.* **1994**, 5, 873–885.
37. Guevremont, R.; Siu, K. W. M.; Wang, J.; LeBlanc, J. C. Y. *Proceedings of the 42nd ASMS Conference on Mass Spectrometry and Allied Topics*, May 29–June 3, 1994, Chicago, IL, p. 999.
38. Carr, S. A.; Huddleston, M. J.; Bean, M. F. *Protein Sci.* **1993**, 2, 183–196.
39. Anacleto, J. F.; Pleasance, S.; Boyd, R. K. *Org. Mass Spectrom.* **1992**, 27, 660–666.
40. Tang, L.; Kebarle, P. *Anal. Chem.* **1993**, 65, 3654–3668.
41. Kostianen, R.; Bruins, A. P. *Rapid Commun. Mass Spectrom.* **1994**, 8, 549–558.
42. Zook, D. R.; Bruins, A. P. *Proceedings of the 42nd ASMS Conference on Mass Spectrometry and Allied topics*, May 29–June 3, 1994, Chicago, IL, p. 1015; *Int. J. Mass Spectrom. Ion Processes*, **1997**, in press.
43. Gomez, A.; Tang, K. *Phys. Fluids* **1994**, 6, 404–414.
44. Kebarle, P.; Tang, L. *Anal. Chem.* **1993**, 65, 972A–986A.

# Mass Spectrometry and Ion Physics

## *EDITORIAL BOARD:*

*R. Baldock (Oak Ridge)*  
*H.D. Beckey (Bonn)*  
*F. Bernhard (Berlin, D.D.R.)*  
*J.H. Beynon (Swansea)*  
*A.J.H. Boerboom (Amsterdam)*  
*C. Brunnée (Bremen)*  
*J.E. Colling (Liège)*  
*N.R. Daly (Aldermaston)*  
*R.E. Honig (Princeton)*

*K.R. Jennings (Coventry)*  
*J. van Katwijk (Amsterdam)*  
*G.W. Kenner (Liverpool)*  
*A.O.C. Nier (Minneapolis)*  
*R.I. Reed (Glasgow)*  
*H.M. Rosenstock (Washington, D.C.)*  
*E. Roth (Gif-sur-Yvette)*  
*J.D. Waldron (East Grinstead)*

Vol. 25 (1977)

ELSEVIER SCIENTIFIC PUBLISHING COMPANY AMSTERDAM

**B 165**

© Elsevier Scientific Publishing Company, 1977.

All rights reserved. No part of this publication may be reproduced, stored in a retrieval system or transmitted in any form or by any means, electronic, mechanical, photocopying, recording or otherwise, without the prior written permission of the publisher, Elsevier Scientific Publishing Company, P.O. Box 330, Amsterdam, The Netherlands.

Submission of an article for publication implies the transfer of the copyright from the author to the publisher and is also understood to imply that the article is not being considered for publication elsewhere.

Printed in The Netherlands

*International Journal of Mass Spectrometry and Ion Physics*, 25 (1977) 129–136 129  
© Elsevier Scientific Publishing Company, Amsterdam — Printed in The Netherlands

## COLLISION-INDUCED DISSOCIATION OF WATER CLUSTER IONS AT HIGH PRESSURE

H. KAMBARA and I. KANOMATA

*Central Research Laboratory, Hitachi, Ltd., Kokubunji, Tokyo (Japan)*

(Received 10 January 1977)

NOTICE: This material may be protected  
by copyright law (Title 17 U.S. Code)

### ABSTRACT

Water cluster ions are reduced to  $\text{H}_3\text{O}^+$  by collision-induced dissociation at ca 1 torr. The cluster ion abundance changes drastically with the electric field strength in the collision region. Collision-induced dissociation takes place through a multiple collision process. The critical field strength for the dissociation is closely related to cluster ion dissociation energy.

### INTRODUCTION

Atmospheric pressure ionization (API) is a new ionization method developed by Horning et al. [1–7]. It is based on ion–molecule reactions at atmospheric pressure, through which small samples can be ionized efficiently. Consequently, the API method has a high sensitivity for trace impurity detection.

In the API ion source, ionization reactions are initiated by electrons emitted from a  $^{63}\text{Ni}$   $\beta$ -ray source or by a corona discharge. A complex sequence of ion–molecule reactions [11–13] takes place in a flowing gas stream at atmospheric pressure. Often many cluster ions are produced from a molecular species [14,15] and it is sometimes difficult to determine what kind of cluster ions they are. Cluster ion formation hampers quantitative and qualitative application of API. Therefore, it is desirable to develop a method which reduces these clusters to their molecular or quasi-molecular ions.

Collision-induced dissociation in a pressure range of ca. 1 torr was applied to distinguish clusters from molecular or quasi-molecular ions in pure nitrogen gas analysis [16]. The collision-induced dissociation method eliminates the drawbacks inherent in API. Cluster ions which have relatively small dissociation energies easily dissociate into smaller cluster ions through collisions with neutral molecules. This occurs as the clusters are accelerated in an electric field.

Collisional dissociations of ions in a pressure range of  $10^{-3}$ – $10^{-4}$  torr have been reported [17,18]. Shahn [19] and Hiraoka [20,21] reported that cluster ions were reduced to simpler ones through collisions with neutral gas

after leaving a high pressure ion source. McLafferty developed a collision activation (CA) technique [22] to investigate energy and structural characteristics of ions, which also utilizes collisional decomposition of ions. These collision-induced dissociations occur in a low pressure region of ca.  $10^{-3}$  torr, in which the mean free path of the ions is ca. 5 cm. Consequently the ion which encounters a neutral molecule dissociates to a simple ion.

On the other hand, cluster ions collide many times with neutral molecules before dissociation at high pressure. This indicates that the dissociation mechanism in the 1-torr region differs from those in a lower pressure region such as  $10^{-3}$  torr.

The collision-induced dissociation of water cluster ions has been investigated at  $\sim 1$  torr. The relationship between cluster ion dissociation energy and field strength in a collision chamber has been studied.

#### EXPERIMENTAL

Cluster ion abundance after collisional dissociation at  $\sim 1$  torr was investigated for various electric field strengths in the collision region. The measurements were made with an API mass spectrometer which is shown in Fig. 1.

A two stage differential pumping system was employed to introduce ions produced at atmospheric pressure into the analyzing region. This is essentially the same apparatus described in a previous paper [16]. The apparatus consists of three parts: an ion source at atmospheric pressure, an intermediate pressure region at  $\sim 1$  torr and an analyzing region at  $10^{-5}$  torr. The intermediate region was used for investigating collision-induced dissociation of cluster ions. A needle electrode produced a corona discharge to supply primary ions. A quadrupole mass spectrometer was used to analyze the resulting ions.

The previous apparatus was modified in the intermediate region. Two aperture electrodes with 0.1- and 0.2-mm diameter apertures separate the intermediate region from the ionization region and the analyzing region,

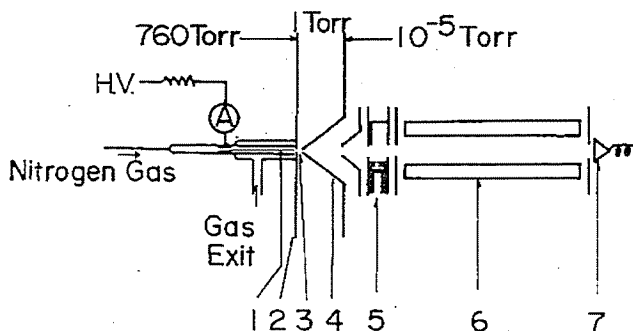


Fig. 1. Schematic diagram of the experimental apparatus: 1) needle electrode, 2) aperture slit (0.1-mm diam.), 3) collision region (intermediate pressure region), 4) aperture slit (0.2-mm diam.), 5) calibration ion source, 6) quadrupole mass analyzer, 7) electron multiplier.

respectively. The second aperture electrode is a cone-shaped electrode with an apex angle of  $90^\circ$ . This arrangement produces such advantages as a slow electric field change along the axis through the first and the second aperture, an ion focusing effect on the second aperture because of a centripetal electric field, and a less likely disturbance of the gas flow during ion sampling [23]. The distance between the two aperture electrodes was 4 mm. The centers of the first and the second apertures were aligned within  $10\ \mu\text{m}$ .

The intermediate region was evacuated with a  $250\text{-l min}^{-1}$  rotary pump. The pressure, monitored with a MacLeod gauge, was 0.7 torr; however, the real pressure in the intermediate region was probably higher. The analyzing region was evacuated to  $1 \times 10^{-5}$  torr using a  $1200\text{-l s}^{-1}$  oil diffusion pump with a cold trap, which gave a real pumping speed of  $200\text{-l s}^{-1}$  at the ion entrance of the mass spectrometer.

Nitrogen gas including water traces was employed as the sample gas. The experiments were done at room temperature. Primary ions,  $\text{N}^+$  and  $\text{N}_2^+$ , produced by the corona discharge react rapidly with nitrogen to give  $\text{N}_3^+$  and  $\text{N}_4^+$ . These ions react further with water to produce cluster ions such as  $\text{H}^+(\text{H}_2\text{O})_n$  ( $n = 1, 2, \dots$ ). Most of these ions are quenched through collisions with the chamber walls; however, some enter the intermediate region through the first aperture.

As will be seen, the cluster ions are accelerated by the electric field in the intermediate region and collide with nitrogen molecules converting a part of their kinetic energy into internal energy. Finally, the excited cluster ions attain enough internal energy to dissociate into simpler ions under a sufficiently large electric field. These dissociated ions enter the analyzing region through the second aperture and are analyzed by the quadrupole mass spectrometer.

The electric potential of the second aperture electrode determines the ion

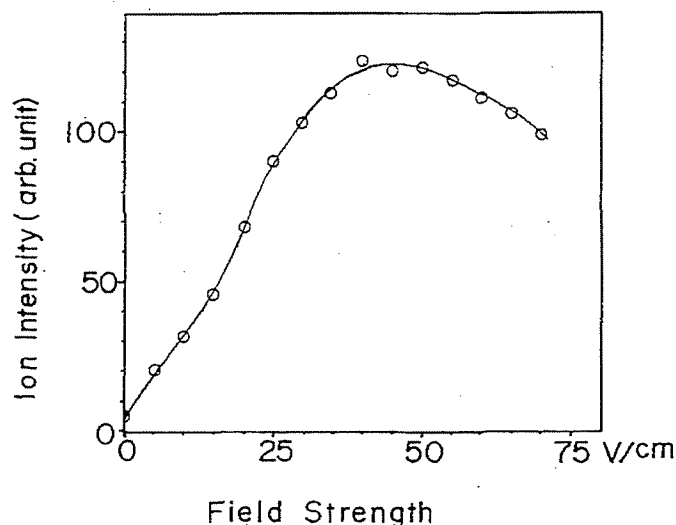


Fig. 2. Total ion intensity change with electric field strength in the collision region.

acceleration energy which was fixed at 3 V. The electric field strength in the intermediate region was varied by changing the electric potential of the first aperture electrode between 3 and 31 V. The total ion current entering the analyzing region depends on the electric field strength in the intermediate region as shown in Fig. 2. This is because ions are focused by the centripetal electric field.

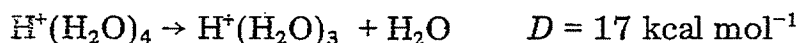
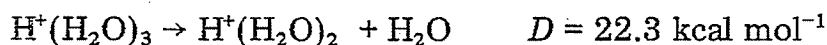
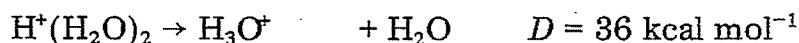
The cluster ion abundance approaches an equilibrium determined by the pressure in the intermediate region. It takes ca. several hundred  $\mu\text{s}$  for the equilibrium between water cluster ions to be established at  $\sim 1$  torr [13]. However, the intermediate region residence time of the cluster ions is estimated to be  $\sim 20$   $\mu\text{s}$  at most. Therefore the pressure equilibrium of the cluster ions cannot be established there. Cluster ion abundance in the ionization region can be maintained also in the intermediate region for a field-free condition if the adiabatic expansion effect [24] on water cluster ion formation is neglected.

## RESULTS AND DISCUSSION

### *Dissociation of Water Cluster Ions*

Relative cluster ion intensities for various electric fields are depicted in Fig. 3. Cluster ions such as  $\text{H}^+(\text{H}_2\text{O})_4$  (73 a.m.u.) were observed in an electric field less than  $20 \text{ V cm}^{-1}$ . The cluster ions began to dissociate into smaller ions as the electric field strength increased in the intermediate region. Ion intensities of  $\text{H}^+(\text{H}_2\text{O})_3$ ,  $\text{H}^+(\text{H}_2\text{O})_2$  and  $\text{H}_3\text{O}^+$  started to increase at electric field strengths greater than 18, 30 and  $50 \text{ V cm}^{-1}$ , respectively. These changes are due to cluster ion dissociation through collision with neutral molecules after acceleration in the electric field. The critical field strength ( $E_c$ ), at which cluster ions started to dissociate, is related to the cluster ion dissociation energy ( $D$ ) \*.

Kebarle et al. [25] reported  $D$  values for water cluster ions as follows



The ratio  $E_c/D$  for each cluster ion is nearly constant. For example, the ratios  $E_c/D$  for ( $n = 4 \rightarrow 3$ ), ( $n = 3 \rightarrow 2$ ) and ( $n = 2 \rightarrow 1$ ) are 1.1, 1.4 and  $1.4 \text{ V mol cm}^{-1} \text{ kcal}^{-1}$ , respectively. This suggests that dissociation energies are closely related to critical field strengths. The ratio  $E_c/D$  for the  $\text{H}^+(\text{H}_2\text{O})_4$  dissociation is smaller than the others. This can be explained by assuming that the  $\text{H}^+(\text{H}_2\text{O})_4$  ion produced in the ion source has a large internal energy.

There are two possible ways in which clusters could come to possess high

\* More exactly,  $E_c$  is related to  $D$ , pressure, cluster size, internal energy of clusters and the intermediate region length.

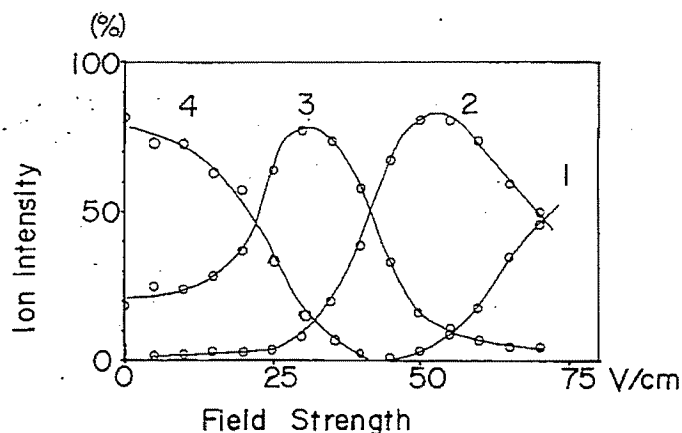


Fig. 3. Change of the cluster ion abundance numbers (1–4) denote the order of the cluster ion ( $n$ ),  $H^+(H_2O)_n$ .

internal energy levels. First, there exists an electric field (ca.  $7.5 \text{ kV cm}^{-1}$ ) in the ion source, which is strong enough to give the ions an energy larger than the thermal energy. The other possibility is that the residence time of clusters produced in the ionization region is so short that the clusters produced are not sufficiently de-excited before entering the intermediate region. In these cases, the dissociation energy ( $D$ ) should be replaced by  $(D - \epsilon)$ , where  $\epsilon$  is the energy related to the excess internal energy. Detailed discussions about the relation between the critical field strength and bond dissociation energy must await further investigation.

#### *Dissociation Mechanism*

The cluster ion dissociation mechanism consists of various factors. Accelerated cluster ions collide with neutral molecules to convert their kinetic energy into internal energy. The cluster ions dissociate if the internal energy increases beyond a critical energy level. There are three probable mechanisms responsible for the dissociation [17].

One is that dissociation occurs by exciting the cluster ions electronically. This mechanism appears frequently in photo- or electron-impact excitation processes. The second is that dissociation is caused by a momentum transfer during a collision, through which cluster ions obtain enough vibrational energy to dissociate. The third process is also the result of vibrational excitation [26]. However in this case, cluster ions can not obtain enough energy from a single collision to dissociate. Cluster ions begin to dissociate only after multiple collisions.

When the pressure in the collision region (intermediate pressure region) is as low as  $10^{-3}$  torr, the probability of multiple collisions is small. Therefore, cluster ions can only dissociate through a single collision, which suggests that the first and the second mechanisms are acceptable for collision-induced dissociation (CID) in a low pressure region. Almost all CID studies reported to date belong to this category.